JOURNAL OF NATURAL PRODUCTS

Article

Cite This: J. Nat. Prod. XXXX, XXX, XXX−XXX

pubs.acs.org/jnp

Water-Soluble Glutamic Acid Derivatives Produced in Culture by *Penicillium solitum* IS1-A from King George Island, Maritime Antarctica

Julie P. G. Rodríguez,[†,#] Darlon I. Bernardi,[†,#] Juliana R. Gubiani,[†] Juliana Magalhães de Oliveira,[‡] Raquel P. Morais-Urano,[†] Ariane F. Bertonha,[†] Karin F. Bandeira,[†] Jairo I. Q. Bulla,[†] Lara D. Sette,[§] Antonio G. Ferreira,[‡] João M. Batista, Jr.,[⊥] Thayná de Souza Silva,[∥] Raquel Alves dos Santos,[∥] Carlos H. G. Martins,[∥] Simone P. Lira,[▽] Marcos G. da Cunha,[○] Daniela B. B. Trivella,[○] Nathalia Grazzia,[¶] Natália E. S. Gomes,[¶] Fernanda Gadelha,[¶] Danilo C. Miguel,[¶] Ana Carolina G. Cauz,[¶] Marcelo Brocchi,[¶] and Roberto G. S. Berlinck*[,†]

[†]Instituto de Química de São Carlos, Universidade de São Paulo, CP 780, CEP 13560-970, São Carlos, SP, Brazil

[‡]Departamento de Química, Universidade Federal de São Carlos, 13565-905, São Carlos, SP, Brazil

[§]Departamento de Bioquímica e Microbiologia, Instituto de Biociências, Universidade Estadual Paulista "Júlio de Mesquita Filho", Campus Rio Claro, Avenida 24-A, 1515, Rio Claro, SP, Brazil

[⊥]Instituto de Ciência e Tecnologia, Universidade Federal de São Paulo, 12231-280, São José dos Campos, SP, Brazil

[∥]Núcleo de Pesquisa em Ciência e Tecnologia, Universidade de Franca, Avenida Dr. Armando Salles Oliveira, 201. Pq. Universitário, 14404-600, Franca, SP, Brazil

[▽]Departamento de Ciências Exatas, Escola Superior de Agricultura Luiz de Queiroz, Universidade de São Paulo, Avenida Pádua Dias, 11, CP 9, Agronomia, CEP 13418-900, Piracicaba, SP, Brazil

[○]Brazilian Biosciences National Laboratory, National Center for Research in Energy and Material, Giuseppe Maximo Scolfaro, 10000, Pólo II de Alta Tecnologia de Campinas, 13083-970 Campinas, SP, Brazil

[¶]Instituto de Biologia, Universidade Estadual de Campinas, CEP 13083-862, Campinas, SP, Brazil

Supporting Information

ABSTRACT: A new method of screening was developed to generate 770 organic and water-soluble fractions from extracts of nine species of marine sponges, from the growth media of 18 species of marine-derived fungi, and from the growth media of 13 species of endophytic fungi. The screening results indicated that water-soluble fractions displayed significant bioactivity in cytotoxic, antibiotic, anti-*Leishmania*, anti-*Trypanosoma cruzi*, and inhibition of proteasome assays. Purification of water-soluble fractions from the growth medium of *Penicillium solitum* IS1-A provided the new glutamic acid derivatives solitumine A (**1**), solitumine B (**2**), and solitumidines A−D (**3**−**6**). The structures of compounds **1**−**6** have been established by analysis of spectroscopic data, chemical derivatizations, and vibrational circular dichroism calculations. Although no biological activity could be observed for compounds **1**−**6**, the new structures reported for **1**−**6** indicate that the investigation of water-soluble natural products represents a relevant strategy in finding new secondary metabolites.

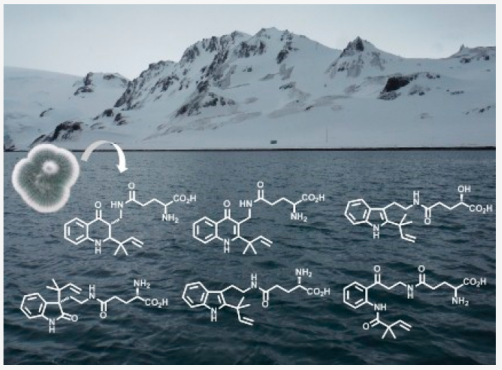

The discovery of structurally novel bioactive secondary metabolites faces the challenge of a steadily decreasing rate in the 21st century.[1−4] Such a landscape raises concerns about the success of biodiscovery programs, in spite of the development of several approaches for the investigation of natural products from both macro- and micro-organisms.[4−6] Biodiscovery redundancy over 50% has been observed by different authors.[1,3] This rather pessimistic outcome for natural products biodiscovery has been, however, questioned by enthusiasts of "omics" technologies, which impressively widened the chemical space of both known and underexplored biological sources.[5−8]

Apparently, no reason justifies worrying natural product chemists and other scientists about the discovery of new bioactive natural products, because only an irrelevant fraction of the biosphere has been chemically scrutinized.[2,6−9] Recent

Received: July 9, 2019

DOI: 10.1021/acs.jnatprod.9b00635
J. Nat. Prod. XXXX, XXX, XXX−XXX

investigations on yet poorly accessed microbial strains, such as Gram-negative bacteria or rare Actinomycetae, clearly demonstrate that microbial secondary metabolite chemical space is far less well-known than was assumed.[6,10−15] Although terrestrial plants have always been a reliable source of structurally unique bioactive natural products,[16,17] in recent years it has been claimed that biodiscovery programs based on terrestrial plants present a very high degree of redundancy.[3] However, the intensive screening of plants from the biodiversity of yet poorly investigated countries such as China,[18] as well as Madagascar, Panama, and Suriname,[16] demonstrates that the structural novelty of bioactive phytochemicals was too early assumed to be exhausted.

One particular aspect that seems to have eluded natural product chemists during the last few decades is a thorough investigation of aqueous-soluble extracts in the search for biologically active metabolites. While bacterial aqueous growth media have been extensively scrutinized during the antibiotics golden age,[19] as well as many water-soluble marine metabolites in the early years of marine natural products biodiscovery,[20−24] the contemporary investigation of water-soluble extracts has been surprisingly less frequent, for unjustified reasons considering the development of state-of-the-art instrumentation and chromatography stationary phases for the separation of hydrophilic compounds.[25−27] A brief overview of the literature shows that the investigation of aqueous extracts from any organism has been largely overlooked for many years.[28−31] Such is the case of fungal growth media, for which only a handful of investigations led to the isolation of water-soluble metabolites during the last 10 years (see below). Considering that all aminoglycosides isolated as potent antibiotics are water-soluble[19] and that several additional water-soluble compounds are reportedly bioactive, such as polyene antibiotics,[32] squalestatins (or zaragozic acids),[33,34] saxitoxins, tetrodotoxins, palytoxins,[6] and phosphonic and phosphinic acids,[35] we envisioned establishing a protocol to obtain water-soluble compounds from aqueous extracts in order to compare bioactivities and chemical profiles with EtOAc-soluble fractions. Subsequent investigation of the water-soluble fraction obtained from the growth medium of the fungus *Penicillium solitum* IS1-A, isolated at the Antarctic continent, provided a series of new glutamic acid derivatives, **1**−**6**, identified by analysis of spectroscopic data and chemical derivatizations. The isolation of the water-soluble **1**−**6** represents 40% of all water-soluble secondary metabolites isolated from fungal cultures since 2008.

RESULTS

A survey of articles published in the *Journal of Natural Products* over the last 10 years (2008−2018) showed that among 500 communications reporting new fungal metabolites ca. 5% used adsorptive stationary phases to capture metabolites from culture media. The remaining 95% of communications reported the isolation of fungal metabolites from EtOAc fractions obtained by liquid−liquid partitioning with culture media (Figure 1). Analysis of procedures reported in articles using adsorptive stationary phases indicated that only three articles reported truly water-soluble metabolites. An additional 20 articles reported compounds isolated using polymeric resin-adsorbing procedures, which, however, did not provide clear evidence that the compounds isolated were water-soluble or not (Supporting Information).

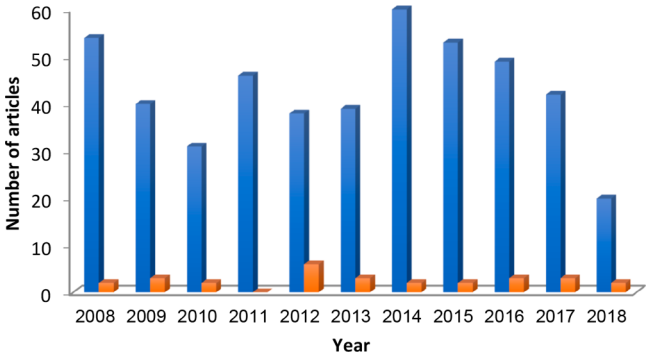

Figure 1. Number of articles published in the *Journal of Natural Products* between 2008 and 2018 reporting fungal metabolites extracted using EtOAc/media partitioning (blue bars) or using solid-phase adsorption (orange bars).

We developed a method for the generation of both organic and water-soluble compound enriched fractions. We prepared a total of 770 fractions for chemical and biological screening. Extracts from nine species of marine sponges, from the growth media of 18 species of marine-derived fungi, and from the growth media of 13 species of endophytic fungi were subjected to this procedure (Scheme 1), summarized as follows.

Scheme 1. Procedure for the Generation of H_2O-Soluble and Organic Fractions Obtained from Marine Sponges and Fungal Culture Media

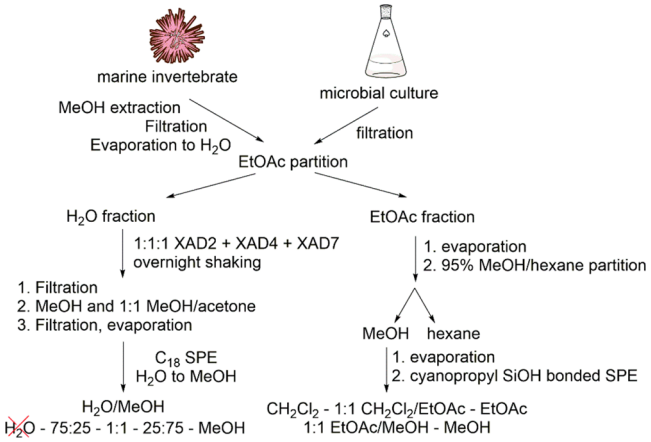

Exhaustive extraction of marine sponges with MeOH provided an extract, which was evaporated and partitioned between EtOAc and H_2O. The dried EtOAc extract was partitioned between 95% MeOH and hexane. The material obtained from evaporation of the 95% MeOH fraction was subjected to a solid-phase extraction on a cyanopropyl-bonded Si cartridge eluted with a gradient of increasing polarity solvent mixtures from CH_2Cl_2 to MeOH, to give five fractions. The water-soluble fractions of sponge MeOH extracts were adsorbed on a 1:1:1 mixture of XAD-2, XAD-4, and XAD-7 macroporous polymeric resins with overnight shaking. The water-soluble organic solutes were desorbed with MeOH and with 1:1 MeOH/acetone, followed by combination and evaporation of organic fractions. The water-soluble organic fraction was then subjected to a C_{18} solid-phase extraction (SPE) eluted with a gradient of MeOH in H_2O, to give five fractions, the first of which (100% H_2O) was discarded (Scheme 1). Filtered fungal

DOI: 10.1021/acs.jnatprod.9b00635
J. Nat. Prod. XXXX, XXX, XXX−XXX

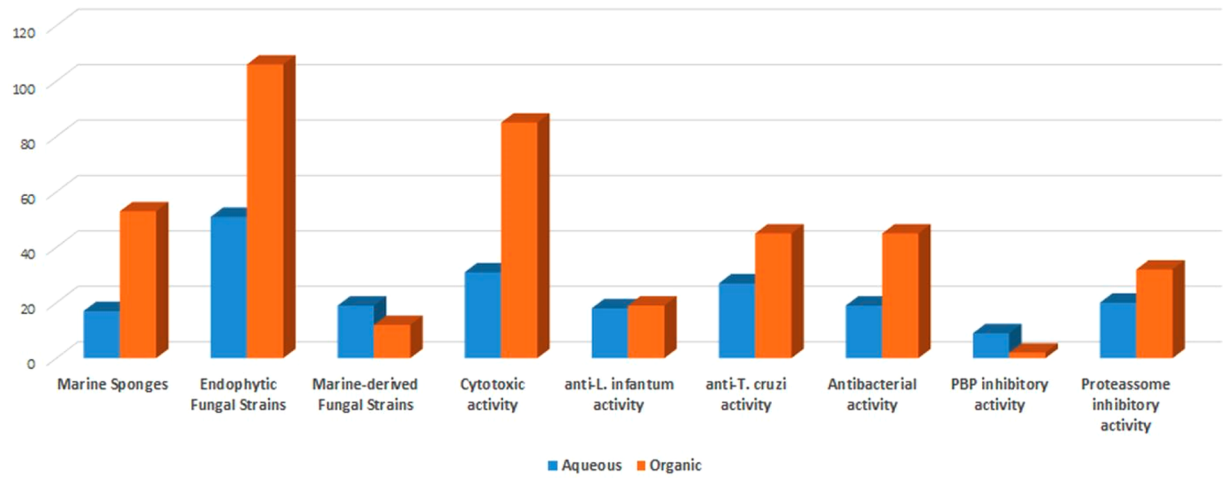

Figure 2. Number of aqueous (blue) and organic (orange) extracts of marine sponges, endophytic fungal strains, and marine-derived fungal strains active in cytotoxic, anti-*L. infantum*, anti-*T. cruzi*, and inhibition of the proteasome inhibitory assays.

Chart 1

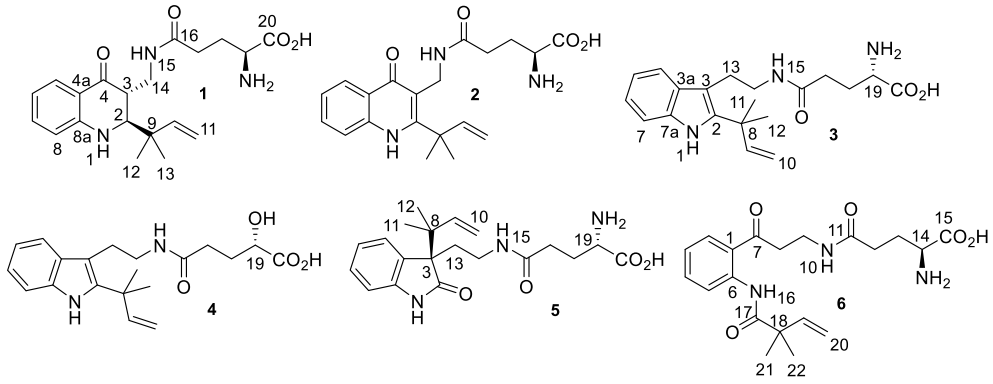

culture media were similarly processed, starting with the EtOAc partition followed by the same procedure.

Of a total of 770 fractions, 454 were obtained from the EtOAc/MeOH-soluble fractions after cyanopropyl-bonded SPE and 316 from the XAD fractions after C_{18} SPE. All fractions were evaluated in bioassays of cytotoxicity on cancer cell lines, antiparasitic activity against *Leishmania* (*L.*) *infantum* and *Trypanosoma cruzi*, antibacterial activity against a panel of resistant microbial pathogenic strains, and inhibition of the yeast 20S proteasome core particle.

The overall results of the biological screening are shown in Figure 2. For marine-derived fungi, a larger number of fractions originated from the XAD C_{18} SPE (named as "aqueous") were active when compared to the fractions originated from the cyanopropyl-bonded SPE of the EtOAc/MeOH fractions (named as "organic"). As for endophytic fungal strains and marine sponges, organic extracts were more active. Organic fractions were active in larger numbers in cytotoxicity, anti-*T. cruzi*, antibacterial, and inhibition of the proteasome assays. The results for antileishmanial assays were comparable for both aqueous and organic fractions. We were pleased to verify that water-soluble fractions were significantly bioactive both in all bioassays and in overall number.

Our screening results are in agreement with a recent evaluation of extracts of 146 marine bacteria strains using Global Natural Product Social Molecular Networking.[36] The authors of this survey[36] observed that 50% of natural product clusters generated by GNPS-Molecular Networking analysis were detected exclusively in polar fractions of marine bacteria media extracted with either MeOH or *n*-BuOH; the remaining 50% of natural product clusters were detected in EtOAc, EtOAc/MeOH, and EtOAc/*n*-BuOH extracts. Our and others'[36] results indicate that very polar compounds constitute a significant portion of secondary metabolism chemical space. We believe that Crüsemann et al.[36] and our results reflect the actual aqueous- vs organic-soluble natural products chemical space, at least from micro-organisms and marine organisms.

Results of our screening indicated that water-soluble fractions obtained from cultures of the marine-derived *Penicillium solitum* IS1-A isolated at the Antarctic Continent displayed cytotoxic activity. Analysis by HPLC-UV-MS of these fractions indicated a series of peaks with varied UV absorptions, such as at λ_{max} 240, 263, and 396 nm, and $[M + H]^+$ signals between m/z 350 and 400. The XAD-desorbed water-soluble fractions obtained after a 5 L and additional 10 L growth of *P. solitum* IS1-A were separated by C_{18} column chromatography, phenyl-derivatized SiOH column chromatography, Sephadex G-15, and purification by HPLC (Supporting Information), to yield compounds **1**–**6**.

Solitumine A (**1**) displayed a $[M + H]^+$ ion in the HRESITOFMS spectrum at m/z 374.2079, corresponding to the formula $C_{20}H_{27}N_3O_4$. Its UV spectrum showed bands at λ_{max} 214, 240, 262, and 396 nm, while the IR spectrum presented a band at 3327 cm^{-1} (broad) for ν_{OH} and ν_{NH} and a

DOI: 10.1021/acs.jnatprod.9b00635
J. Nat. Prod. XXXX, XXX, XXX−XXX

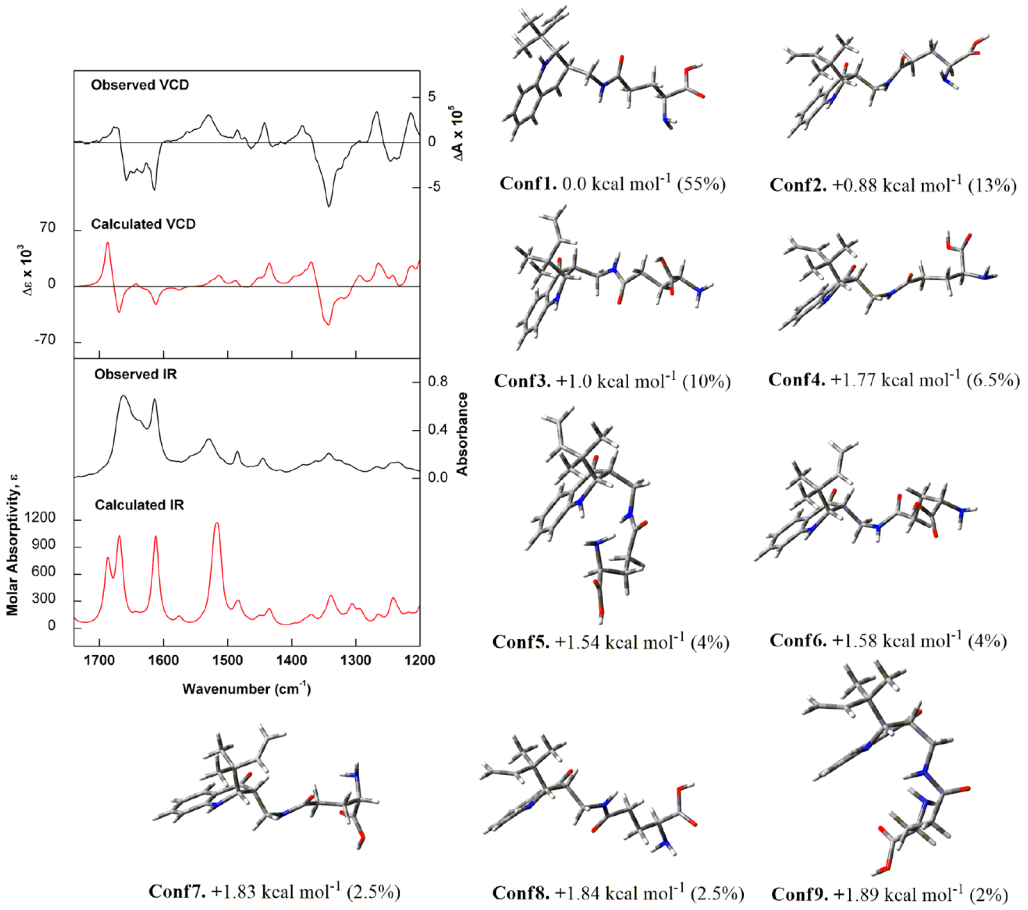

Figure 3. (Left) Comparison of experimental IR and VCD spectra of (+)-**1** recorded in DMSO-d_6 (black trace) with calculated [B3LYP/PCM(DMSO)/6-31G(d)] IR and VCD spectra for the Boltzmann average of the nine lowest-energy conformers identified for (2*S*,3*R*,19*S*)-**1** (red trace). (Right) Optimized structures, relative energies, and Boltzmann populations of the lowest-energy conformers identified for (2*S*,3*R*,19*S*)-**1**.

band at 1665 cm^{-1} for an amide functionality. The ^{13}C NMR spectrum showed signals of aromatic carbons at δ_C 115.5 (C-4a), 126.4 (C-5), 115.0 (C-6), 135.5 (C-7), 115.1 (C-8), and 151.0 (C-8a), a conjugated ketone carbonyl at δ_C 193.9 (C-4), and two carboxylic groups at δ_C 172.6 (C-16) and 171.0 (C-20). Analysis of ^1H, ^{13}C, and HSQC NMR spectra evidenced a terminal double bond with chemical shifts at δ_H 5.62 (dd, 17.1, 11.1; δ_C 144.8, CH-10) and δ_H 4.87 (dd, 11.1, 1.1) and 4.86 (dd, 17.1, 11.1; δ_C 113.1, CH_2-11). Signals of methylene groups were observed at δ_H 3.10 (CH_2-14), 2.26 (CH_2-17), and 1.94/1.87 (CH_2-18), of methines at δ_H 3.17 (δ_C 59.7, CH-2), δ_H 2.63 (δ_C 46.3, CH-3), and δ_H 3.30 (δ_C 54.0, CH-19), of a nonprotonated carbon at δ_C 43.0 (C-9), and of singlet methyl groups at δ_H 0.91 (δ_C 24.8, Me-12) and δ_H 0.83 (δ_C 22.9, Me-13). Analysis of the ^1H and COSY NMR spectra indicated a 1,2-disubstituted benzene moiety from CH-5 to CH-8, a CH–CH_2 fragment (CH-3 and CH_2-14), and a CH_2–CH_2–CH fragment (CH_2-17, CH_2-18, and CH-19). Data from the HMBC spectrum revealed a reverse prenyl group attached at CH-2. Correlations were detected for the *gem*-dimethyl group δ_H 0.91 (δ_C 24.8, C-12) and δ_H 0.83 (δ_C 22.9, C-13) to CH-2, C-9, CH-10, and CH_2-11. The H-2 methine showed a vicinal coupling with the NH-1 at δ_H 7.13 (d, 3.0 Hz). Both NH-1 and H-2 presented HMBC correlations with C-8a (δ_C 151.0) and with C-9. Moreover, NH-1, H-2, H-3, H-5, and H_2-14 showed correlations with the conjugated ketone carbonyl at δ_C 193.9 (C-4). Therefore, a 2,3-dihydroquinolin-4(1*H*)-one moiety was defined, substituted at CH-2 by a reverse prenyl group. HMBC correlations of H_2-14, NH-15 (δ_H 8.38, t, 5.7), and H_2-17 (δ_H 2.26, m) with the amide carbonyl at δ_C 172.6 established a connection between the bicyclic moiety and the glutamic acid moiety, constituted of CH_2-17, CH_2-18, CH-19, and the CO_2H group at δ_C 171.0. Thus, the planar structure of **1** was defined. The absolute configuration of the glutamic acid fragment was determined as 19*S* after hydrolysis of **1** and Marfey's analysis.

Although H-2 (δ_H 3.17, brd, J = 4.0 Hz) and H-3 (δ_H 2.63, t, J = 7.6 Hz) did not show vicinal coupling in the ^1H or COSY spectrum, the NOESY spectrum clearly indicated a NOE between H-2 and H-3 (Figure S12, Supporting Information). Considering the HMBC correlations observed for carbons and hydrogens of the dihydroquinolin-4(1*H*)-one moiety, H-2 and H-3 were vicinally placed. A ϕ = 90° dihedral angle between H-2 and H-3 accounted for the absence of vicinal coupling. In order to unambiguously establish the absolute configuration of C-2 and C-3, vibrational circular dichroism (VCD) calculations were performed and compared to experimental data. Initially, calculations were performed for the two possible diastereomers of the 2,3-dihydroquinolin-4(1*H*)-one moiety. The lowest-energy conformers identified for the 2*S*,3*R* stereoisomer indicated a ϕ = 80° approximate dihedral angle between H-2 and H-3, in agreement with the ^1H NMR data. Results of calculations for the 2*R*,3*R* stereoisomer indicated a ϕ = 55° approximate dihedral angle. Once the relative configuration was established as 2*S**,3*R**, calculations were performed for both 2*S*,3*R*,19*S* and 2*R*,3*S*,19*S* (Figure S44).

DOI: 10.1021/acs.jnatprod.9b00635
J. Nat. Prod. XXXX, XXX, XXX−XXX

Excellent agreement was observed between recorded and simulated [B3LYP/PCM(DMSO)/6-31G(d)] IR and VCD spectra for the 2*S*,3*R*,19*S* stereoisomer (Figure 3). These results enabled us to unambiguously assign the absolute configuration of the 2,3-dihydroquinolin-4(1*H*)-one moiety of (+)-**1** as 2*S*,3*R*. Despite the same configuration at C-19, the simulated VCD spectra for 2*S*,3*R*,19*S* and 2*R*,3*S*,19*S* presented almost a mirror-image relationship, indicating the VCD properties to be dominated by the configuration of the 2,3-dihydroquinolin-4(1*H*)-one moiety. The poorer agreement with experimental data observed for (2*R*,3*R*,19*S*)-**1** (Figure S44) further supports the above-mentioned assignment.

Solitumine B (**2**) displayed a $[M + H]^+$ ion in the HRESITOFMS spectrum at *m*/*z* 372.1922, corresponding to the formula $C_{20}H_{25}N_3O_4$, with one more unsaturation than **1**. Its UV spectrum indicated a highly conjugated chromophore, with bands at λ_{max} 214, 240, 247, 318, and 330 nm. The ^1H and ^{13}C NMR spectra of **2** were very similar to those of **1**, except for the missing signals of H-2 and H-3 and for the presence of two additional sp^2 nonprotonated carbons at δ_C 158.7 (C-2) and 116.8 (C-3). The data indicated that **2** was the quinolin-4(1*H*)-one derivative of **1**, a hypothesis confirmed by analysis of HSQC, COSY, and HMBC spectra (Table 1). The absolute configuration at C-19 was established as *S* by Marfey's analysis.

Solitumidine A (**3**) displayed a $[M + H]^+$ ion in the HRESITOFMS spectrum at *m*/*z* 358.2139, corresponding to the formula $C_{20}H_{27}N_3O_3$. Its UV spectrum showed bands at λ_{max} 225, 283, and 291 nm, while the IR spectrum presented bands at 1674 and 1627 cm^{-1} for amide functionalities. The presence of an indole moiety was confirmed by analysis of HSQC, COSY, and HMBC spectra (Table 2). The indole NH-1 at δ_H 10.47 (s) showed HMBC correlations to C-2 (δ_C 140.2), C-3 (δ_C 107.2), C-3a (δ_C 129.3), CH-7 (δ_C 117.8), and C-7a (δ_C 134.8). A reverse prenyl fragment [C-8 (δ_C 38.9), CH-9 (δ_H 6.12, dd, 17.3 and 10.6; δ_C 146.4), CH_2-10 (δ_H 5.03, dd, 17.3 and 1.0 Hz and 5.01, dd, 10.6 and 1.0 Hz; δ_C 111.1), CH_3-11 and CH_3-12 (δ_H 1.48, s; δ_C 28.0)] was attached to C-2 by HMBC correlations observed from H-9, Me-11, and Me-12 to C-2. A two-methylene spin system constituted of CH_2-13 (δ_H 2.86, dd, 8.3 and 7.4 Hz; δ_C 25.5) and CH_2-14 (δ_H 3.17, m; δ_C 39.9) showed HMBC correlations to C-3. Analysis of the COSY spectrum placed CH_2-14 vicinally to NH-15 (δ_H 8.29, t, 5.0 Hz). As observed for solitumines A (**1**) and B (**2**), NH-15 was connected to a glutamic acid moiety by analysis of HMBC correlations of NH-15 and CH_2-17 (δ_H 2.29, m; δ_C 32.1) to the amide carbonyl C-16 (δ_C 172.1). Marfey's analysis of the glutamic acid moiety of **3** defined its absolute configuration as 19*S*.

Solitumidine B (**4**) displayed a $[M + H]^+$ ion in the HRESITOFMS spectrum at *m*/*z* 359.1968, corresponding to the formula $C_{20}H_{26}N_2O_4$, with one less nitrogen atom and one additional oxygen atom than **3**. The NMR data of **4** showed good similarity to those of **3**, except for the glutamic acid moiety, which was shown to be a 2-hydroxyglutaric acid residue (Table 2). The ^1H and ^{13}C NMR signals of CH-19 (δ_H 3.88, dd, 4.4 and 7.6 Hz; δ_C 69.5) completely agreed with this assignment. The assignment of the absolute configuration of 2-hydroxyglutaric acid by chemical derivatization and/or by NMR analysis is not simple.[37−39] After recording the electronic circular dichroism spectra of **3** and **4** (Figures S22 and S28), we could observe positive Cotton effects for solitumidines A and B at λ_{max} 380 and 400 nm, respectively. Since $\Delta\varepsilon$ observed for compound **4** was also of small magnitude, the 19*S* configuration indicated for **4** is suggestive only.

Solitumidine C (**5**) displayed a $[M + H]^+$ ion in the HRESITOFMS spectrum at *m*/*z* 374.2077, corresponding to the formula $C_{20}H_{27}N_3O_4$, the same as compound **1**. However, the UV spectrum of **5** was significantly distinct from those of compounds **1**−**4**, with bands at λ_{max} 208, 251, and 285 nm. A 2-oxindole moiety was observed in **5**, by correlations of NH-1 (δ_H 10.44, s) and CH_2-13 (δ_H 1.98, m; δ_C 30.4) with the lactam carbonyl at C-2 (δ_C 179.3). Indole C-3 (δ_C 56.1) was shown to be substituted by C-8 (δ_C 41.2) and by CH_2-13 (δ_H 1.98, m; δ_C 30.4). Indole C-3 showed HMBC correlations to H-4, H-5, H-7, H_3-11, H_3-12, H_2-13, and H_2-14. A reverse prenyl group was constituted by C-8 (δ_C 41.2), CH-9 (δ_H 6.02, dd, 17.4 and 10.8 Hz; δ_C 143.3), CH_2-10 [δ_H 5.03 (dd, 1.4 and 10.8 Hz) and 4.92 (dd, 17.4, 1.4 Hz); δ_C 113.2], CH_3-11 (δ_H 1.02, s; δ_C 22.1), and CH_3-12 (δ_H 0.94, s; δ_C 21.3). The ethylamide group constituted by CH_2-13, CH_2-14 (δ_H 2.40, m; δ_C 35.3), NH-15 (δ_H 7.89, t, 5.4 Hz), and CO-16 (δ_C 170.3) was connected to a glutamic acid moiety, as observed for compounds **1**−**4**, and the planar structure of solitumidine C (**5**) could be defined. While the absolute configuration of CH-19 of compound **5** was defined as *S* by Marfey's analysis, the absolute configuration at C-3 was established by VCD spectroscopy. Calculations were performed for both *R* and *S* configurations at C-3. The best agreement between calculated and experimental data recorded in DMSO-d_6 was observed for the *R* configuration at C-3 (Figure 4 and Figure S45). Thus,

Table 1. NMR Spectroscopic Data (^1H 600 MHz, ^{13}C 150 MHz) for Solitumine A (1) (DMSO-d_6) and Solitumine B (2) (MeOH-d_4)

	solitumine A (**1**)		solitumine B (**2**)	
position	δ_C, type	δ_H (*J* in Hz)	δ_C, type	δ_H (*J* in Hz)
NH-1		7.13, d (3.0)		
2	59.7, CH	3.17, d (4.0)	158.7, C	
3	46.3, CH	2.63, t (7.6)	116.8, C	
4	193.9, C		180.7, C	
4a	115.5, C		125.1, C	
5	126.4, CH	7.39, dd (8.0, 1.6)	126.0, CH	8.20, dd (8.1, 1.0)
6	115.0, CH	6.42 ddd (8.0, 7.0, 1.0)	125.7, CH	7.40, ddd (8.1, 7.0, 1.0)
7	135.5, CH	7.19 ddd (8.5, 7.0, 1.6)	133.6, CH	7.68, ddd (8.4, 7.0, 1.4)
8	115.1, CH	6.80 d (8.5)	120.1, CH	7.87, d (8.3)
8a	151.0, C		140.8, C	
9	43.0, C		44.6, C	
10	144.8, CH	5.62, dd (17.1, 11.1)	146.6, CH	6.22, dd (17.5, 10.6)
11	113.1, CH_2	4.87, dd, (11.1, 1.1); 4.86, dd, (17.1, 1.1)	114.1, CH_2	5.16, d (10.6) 5.13, d (17.5)
12	24.8, CH_3	0.91, s	28.5, CH_3	1.62, s
13	22.9, CH_3	0.83, s	28.5, CH_3	1.62, s
14	40.7, CH_2	3.10, dd (7.5, 7.0)	38.3, CH_2	4.43, s
NH-15		8.38, t (5.7)		
16	172.6, C		174.9, C	
17	32.1, CH_2	2.26 (m, 2H)	33.4, CH_2	2.39, t (7.0)
18	27.5, CH_2	1.94 (m); 1.87 (m)	28.6, CH_2	2.12 (m); 2.06 (m)
19	54.0, CH	3.30, t (5.9)	56.1, CH	3.57 (m)
20	171.0, C		174.5, C	

DOI: 10.1021/acs.jnatprod.9b00635
J. Nat. Prod. XXXX, XXX, XXX−XXX

Table 2. NMR Spectroscopic Data (^{1}H 600 MHz, ^{13}C 150 MHz, DMSO-d_6) for Solitumidines A–C (3–5)

	solitumidine A (3)		solitumidine B (4)		solitumidine C (5)	
position	δ_C, type	δ_H (J in Hz)	δ_C, type	δ_H (J in Hz)	δ_C, type	δ_H (J in Hz)
NH-1		10.47, s		10.42, s		10.44, s
2	140.2, C		140.1, C		179.3, C	
3	107.2, C		107.2, C		56.1, C	
3a	129.3, C		129.2, C		129.7, C	
4	111.1, CH	7.30, d (8.0)	111.0, CH	7.29, d (8.0)	125.3, CH	7.15, bd (7.7)
5	118.4, CH	6.92, ddd (7.1, 8.3, 1.0)	118.3, CH	6.93, ddd (8.0, 7.0, 1.0)	120.7, CH	6.95, ddd (7.7, 7.6, 1.1)
6	120.5, CH	6.98, ddd (7.1, 8.3, 1.0)	120.5, CH	6.99, ddd (8.0, 7.0, 1.0)	127.8, CH	7.18, ddd (7.7, 7.6 1.1)
7	117.8, CH	7.49, d (7.8)	117.7, CH	7.48, d (8.0)	109.0, CH	6.82, d (7.7)
7a	134.8, C		134.8, C		142.7, C	
8	38.9, C		38.8, C		41.2, C	
9	146.4, CH	6.12, dd (17.3, 10.6)	146.4, CH	6.13, dd (17.2, 10.6)	143.3, CH	6.02, dd (17.4, 10.8)
10	111.1, CH_2	5.03, dd (17.3, 1.0); 5.01, dd (10.6, 1.0)	111.0, CH_2	5.04, dd (17.2, 1.3); 5.03, dd (10.6, 1.3)	113.2, CH_2	5.03, dd (10.8, 1.4); 4.92, dd (17.4, 1.4)
11	28.0, CH_3	1.48, s	27.9, CH_3	1.48, s	22.1, CH_3	1.02, s
12	28.0, CH_3	1.48, s	27.9, CH_3	1.48, s	21.3, CH_3	0.94, s
13	25.5, CH_2	2.86, dd (7.4, 8.3)	25.5, CH_2	2.83, m	30.4, CH_2	1.98, m
14	39.9, CH_2	3.17, m	38.8, CH_2	3.16, m	35.3, CH_2	2.40, m
NH-15		8.29, t (5.0)		8.00, t (5.7)		7.89, t (5.4)
16	172.1, C		171.8, C		170.3, C	
17	32.1, CH_2	2.29, m	31.5, CH_2	2.15, m	30.4, CH_2	2.21, m; 2.12, m
18	27.3, CH_2	1.99, m; 1.91, m	30.2, CH_2	1.92, m; 1.68, m	25.7, CH_2	1.93, m
19	53.9, CH	3.32, bt (5.4)	69.5, CH	3.88, dd (7.6, 4.4)	51.5, CH	3.83, m
20	170.7, C		175.8, C		170.6, C	
NH-21						8.37, s

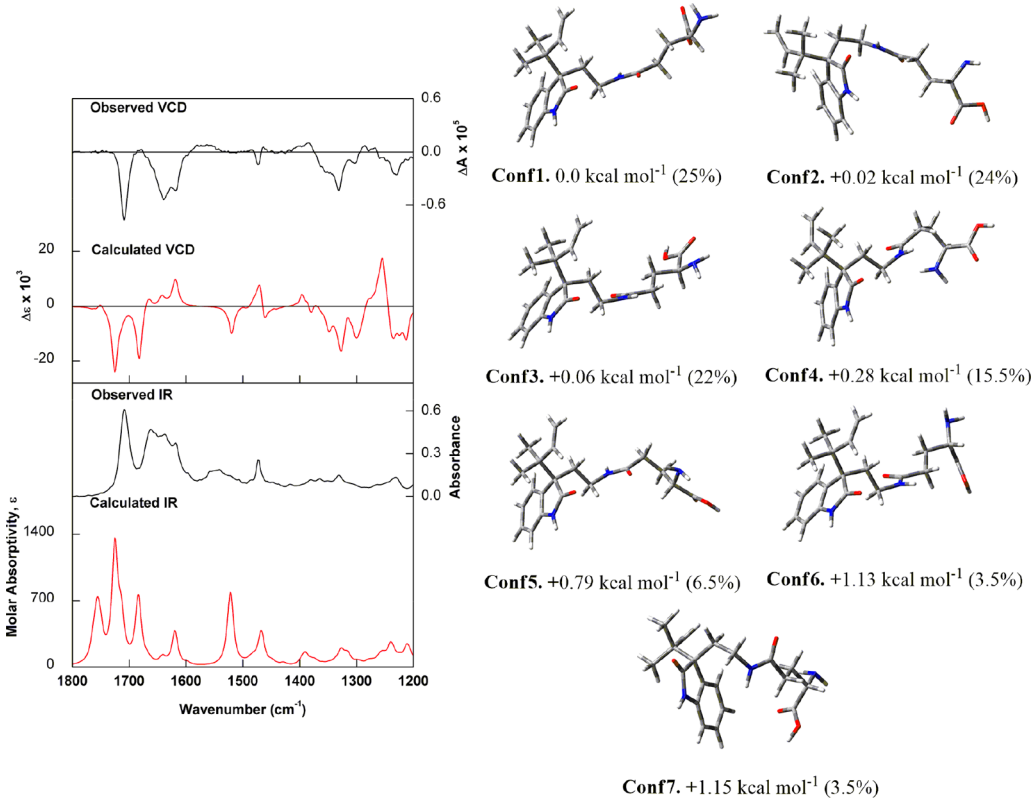

Figure 4. Left: Comparison of the observed IR and VCD spectra of (−)-5 recorded in DMSO-d_6 (black trace) with the calculated [B3LYP/PCM(DMSO)/6-31G(d)] IR and VCD spectra for the Boltzmann average of the seven lowest-energy conformers identified for (3*R*,19*S*)-5 (red trace). Right: Optimized structures, relative energies, and Boltzmann populations of the lowest-energy conformers identified for (3*R*,19*S*)-5.

the absolute configuration of compound (−)-5 was established as 3*R*,19*S*.

Solitumidine D (6) displayed a $[M + H]^+$ ion in the HRESITOFMS spectrum at m/z 390.2010, corresponding to

DOI: 10.1021/acs.jnatprod.9b00635
J. Nat. Prod. XXXX, XXX, XXX−XXX

the formula $C_{20}H_{27}N_3O_4$, with nine double-bond equivalents. Its UV spectrum displayed bands at λ_{max} 231, 234, 261, 267, and 327 nm. Its IR spectrum presented bands at 3408 (ν_{O-H}), 1730, and 1658 ($\nu_{C=O}$) cm^{-1}. NMR data of **6** indicated it as a 1,2-disubstituted benzene derivative (Table 3), with signals

Table 3. NMR Spectroscopic Data (^1H 600 MHz, ^{13}C 150 MHz, MeOH-d_4) for Solitumidine D (6)

position	δ_C, type	δ_H (J in Hz)
1	124.2, C	
2	132.6, CH	8.04, dd (8.2, 1.3)
3	124.4, CH	7.19, ddd (8.2, 7.3, 1.3)
4	136.0, CH	7.56, ddd (8.5, 7.3, 1.0)
5	122.2, CH	8.58, dd (8.5, 1.0)
6	141.7, C	
7	204.5, C	
8	40.5, CH	3.31, t (6.7)
9	36.5, CH_2	3.57, t (6.5)
NH-10		
11	174.5, C	
12	32.7, CH_2	2.45, td (7.2, 1.4)
13	27.4, CH_2	2.17, m; 2.10, m
14	53.8, CH	4.01, t (6.3)
15	171.7, C	
NH-16		
17	178.0, C	
18	48.1, C	
19	143.9, CH	6.12, dd (17.4, 10.7)
20	115.6, CH_2	5.34, dd (17.4, 0.5); 5.28, dd (10.7, 0.5)
21	25.4, CH_3	1.39, s
22	25.4, CH_3	1.39, s

assigned to CH-2 at δ_H 8.04 (dd, 8.2, 1.3; δ_C 132.6), CH-3 at δ_H 7.19 (ddd, 8.2, 7.3, 1.3; δ_C 124.4), CH-4 at δ_H 7.56 (ddd, 8.5, 7.3, 1.0; δ_C 136.0), and CH-5 at δ_H 8.58 (dd, 8.5 and 1.0; δ_C 122.2). Four carbonyl groups were observed at δ_C 204.5 (C-7), 174.5 (C-11), 171.7 (C-15), and 178.0 (C-17). Analysis of COSY, HSQC, and HMBC spectra positioned a 2,2-dimethylbut-3-enamide group attached to the benzene moiety, with vicinal couplings observed for the vinyl hydrogens at δ_H 6.12 (dd, 17.4 and 10.7, H-19), 5.34 (dd, 17.4 and 0.5, H-20a), and 5.28 (dd, 10.7 and 0.5, H-20b), and long-range $^1H-^{13}C$ couplings between the vinylic hydrogens and C-6, as well as between the methyl groups Me-21 and Me-22 at δ_H 1.39 (s; δ_C 25.4) with C-6 and the vinyl carbons at δ_C 143.9 (C-19) and 115.6 (C-20). A second spin system was constituted by CH_2-8 at δ_H 3.31 (t, 6.7; δ_C 40.5) and CH_2-9 at δ_H 3.57 (t, 6.5; δ_C 36.5). Since H_2-8 showed HMBC couplings with the ketone carbonyl C-7 and with C-6 (δ_C 141.7), while H_2-9 showed HMBC couplings with C-7 and with the carboxylic group at δ_C 174.5 (C-11), a Ph−(CO)−CH_2−CH_2−NH(CO) moiety was assigned to this subunit. The final structure of **6** was established by analysis of COSY and HMBC spectra by comparison with data of compounds **1**−**5**, the remaining portion assigned to a glutamic acid residue. The absolute configuration of the glutamic acid moiety was established as *S* by hydrolysis and Marfey's analysis.

Following the successful isolation of the water-soluble glutamic acid derivatives **1**−**6** from cultures of *P. solitum* IS1-A, we decided to investigate which of the XAD resins better captured these metabolites from the aqueous fraction. A quantitative adsorption−desorption analysis of **1** was performed, measuring its recovery from XAD-2, XAD-4, and XAD-7 resins, separately.

A calibration curve (Figure S1) was constructed by plotting the areas (y) of the chromatographic peak of **1** against the corresponding standard concentration (x), using a linear least-squares fit regression ($y = 2.0 \times 10^7 x + 29\,680$). The correlation coefficient (R^2) was 0.9997 in concentration ranges of **1** between 0.01 and 0.18 mg mL^{-1}. Quantitative analyses included sample stability, method precision, and relative standard deviations (%RSD) for intraday and interday precision with values smaller than 5.8% (Supporting Information). The validated method was applied to the quantification of solitumine A (**1**), in triplicate after three independent *P. solitum* ISA-1 growth experiments. Compound **1** was consistently detected only in the 1:1 H_2O/MeOH fraction from the SPE of the desorbed organic material obtained from each of the XAD-2, XAD-4, and XAD-7 resins, separately for each of the growth experiments. Student's t test indicated that the p parameter was less than 0.05, representing statistically significant differences between the four C_{18} reversed-phase fractions (25% MeOH, 50% MeOH, 75% MeOH, and 100% MeOH) eluted from the XAD-2, -4, and -7 desorbed organic material. The results obtained indicate that the C_{18} reversed-phase SPE of the XAD-desorbed organic material is very efficient in concentrating distinct analytes in the different SPE fractions. Figure S2 shows concentration values of solitumine A (**1**) in each of the four fractions eluted from XAD-2. Solitumine A (**1**) is far more abundant in the SPE fraction 1:1 H_2O/MeOH. Very similar results were obtained for the quantification experiments performed with XAD-4 and XAD-7.

We expected that one of the three macroporous polymer resins would be more selective for the adsorption of compound **1**, because for XAD resins the adsorption of analytes is polarity dependent.[21,40,41] Nevertheless, not only were individual HPLC-UV-MS chromatograms recorded for each of the SPE 1:1 MeOH/H_2O fractions of the XAD organic desorbed material from each of the resins practically identical (Figure S3, Supporting Information), but also the concentration of solitumine A (**1**) was almost the same in the SPE 1:1 MeOH/H_2O fractions obtained from either XAD-2, XAD-4, or XAD-7 resins: 93, 103, and 115 mg g^{-1} of resin, respectively (Figure S4). The concentration of **1** in the other SPE fractions (25% MeOH, 75% MeOH, and 100% MeOH) was negligible. Therefore, solitumine A (**1**) was captured in the same relative amount by XAD-2, XAD-4, and XAD-7 macroporous resins (Figure S4). When the Student's t test was applied to compare the fractions that contained **1** desorbed from each of the XAD resins, no statistically significant difference was observed ($p > 0.05$).

We consider that the nonselective adsorption of **1** by XAD-2, XAD-4, and XAD-7 can be explained because solitumine A has both apolar (aromatic) and polar (glutamic acid) moieties that influence its adsorption by the macroporous resins and also because the three resins can capture compounds in the molecular weight range of **1**.

Different adsorptive XAD resins are commonly used to capture water contaminants.[42] Comparisons on the adsorption capabilities of XAD resins have been performed for different classes of natural products.[40] Several parameters, such as microporous resin specific surface area, pore diameter, resin polarity, and polarity of adsorbates, play a significant role in the properties of adsorptive resins.[43] The use of macroporous

DOI: 10.1021/acs.jnatprod.9b00635
J. Nat. Prod. XXXX, XXX, XXX−XXX

polymeric resins for the adsorption of secondary metabolites released by microbes in culture media is well documented.[44−47] However, no investigation has been specifically performed for water-soluble microbial metabolites. Quinn[21] authoritatively discusses the advantages of using XAD resins for the isolation of water-soluble metabolites from aqueous extracts of marine organisms. Based on Quinn's considerations,[21] we have employed XAD resins for the isolation of metabolites from marine invertebrates on different occasions[48−50] and more recently in the isolation of microbial metabolites.[51,52] The use of adsorptive resins constitutes a reliable strategy for improving the yields of microbial production in culture, such as for epothilone D.[47,53]

A partition between EtOAc and H_2O of a MeOH extract from marine sponges, or between EtOAc and culture media, provided fractions with constituents of clearly distinctive polarity. At least in one case we observed that compounds extracted with EtOAc were also present in the H_2O fraction, in even higher concentration. It seems that compounds that may be considered as minor constituents in an EtOAc fraction can be major in the corresponding H_2O-soluble fraction and can be missed if investigation of the H_2O-soluble fraction is not performed. One strategy to overcome this problem is the adsorption of the whole filtered growth media in adsorptive resins or a solid phase extraction of a whole organismal extract instead of performing a liquid partitioning procedure. Indeed, several reports adopt such procedures (Supporting Information). Possible drawbacks of such an approach are (1) rapid saturation of stationary phases, mainly with large amounts of apolar compounds, and (2) difficulty to subsequently separate mixtures containing both polar and apolar constituents. Our approach provided fractions of distinct polarity, which are easier to subsequently separate by column chromatography and by HPLC.

We observed that desorption of microbial water-soluble metabolites from the XAD-2, -4, and -7 resin mixture provided a fraction still containing significant amounts of growth media constituents. Chromatography of the XAD-desorbed material on a C_{18} reversed phase column[54] is effective to remove such contaminants and provide much cleaner water-soluble fractions suitable for hyphenated HPLC dereplication and bioassay testing. We tested a previously reported prefractionation strategy using C_{18} reversed-phase chromatography,[55,56] for the separation of water-soluble compounds previously not adsorbed on polymeric XAD resins. However, this procedure yielded fractions still heavily contaminated with media constituents. Combination of XAD adsorption/desorption followed by C_{18} reversed-phase chromatography of water-soluble material proved to be suitable in providing clean material for chemical and biological screening and, after scaling up, for isolation of water-soluble compounds. In a preparative scale, with large amounts of media contaminants, a third separation step using gel-filtration on either Sephadex LH-20 (with MeOH or 1:1 MeOH/H_2O), Sephadex G-10 or G-15 (with 9:1 H_2O/MeOH), or BioGel P-2 (with 8:2 H_2O/EtOH) or even a reversed-phase separation on a cyanopropyl-bonded Si gel chromatography column (gradient of MeOH in H_2O) provided water-soluble fractions essentially free of media constituents. The isolation of the new glutamic acid derivatives **1**−**6** constitutes a proof-of-concept that investigation of purely water-soluble fractions may significantly contribute to the discovery of new chemical scaffolds.

The isolation of γ-derivatized glutamic acid derivatives **1**−**6** is of interest, because many related compounds are of pharmacological and nutraceutical economic importance.[57,58] The dipeptide γ-D-glutamyl-L-tryptophan (SCV-07) is an immunomodulating agent that improves the treatment of tuberculosis and stimulates the proliferation of thymic and splenic cell proliferation.[59] SCV-07 also suppresses tumor growth and reduces side effects of chemoradiation therapy.[60] SciClone Pharmaceuticals Inc. and Soligenix, Inc. reported positive results of SCV-07 phase II clinical trials.[61] Therapeutically and economically relevant γ-glutamate derivatives are enzymatically produced by γ-glutamyl transpeptidases.[62]

We tested compounds **1**−**6** in cytotoxicity and antibacterial assays against several cancer cell lines, Gram-negative and Gram-positive pathogens, but none of the compounds showed activity, possibly due to a self-fluorescence for **1**−**5**. *P. solitum* glutamic acid derivatives are herein reported for the first time as secondary metabolites. Our results clearly indicate that investigation of fungal culture media water-soluble metabolites should be seriously considered in future biodiscovery programs, as it has been also recently proposed for the NCI Program for Natural Product Discovery.[63]

EXPERIMENTAL SECTION

General Experimental Procedures. Optical rotations were recorded on a Polartronic H Schmidt+Haensch polarimeter. UV spectra were recorded on a Shimadzu UV-3600 spectrophotometer. IR and VCD spectra of compounds **1** and **5** were recorded with a Single-PEM Chiral*IR*-2X FT-VCD spectrometer (BioTools, Inc.) using a resolution of 4 cm^{-1} and a collection time of 6 h. The optimum retardation of the ZnSe photoelastic modulator (PEM) was set at 1400 cm^{-1}. Minor instrumental baseline offsets were eliminated from the final VCD spectra of **1** and **5** by subtracting each VCD spectra from that obtained for the solvent under identical conditions. The IR and VCD spectra were recorded in a BaF_2 cell with 100 μm path length using DMSO-d_6 as solvent. The samples were prepared as follows: 4.7 mg of **1** in 150 μL of DMSO-d_6 and 6 mg of **5** in 150 μL of DMSO-d_6: IR spectra were obtained on a Shimadzu IRAffinity-1 Fourier transform infrared spectrophotometer on a silica plate. NMR spectra were obtained at 25 °C, with tetramethylsilane as an internal standard, using a Bruker AV-600 spectrometer operating at either 600 MHz (^{1}H) or 150 MHz (^{13}C) with a 2.5 mm cryoprobe. The acquisition of high-resolution mass spectra (HRMS) in the centroid MS mode was performed in a positive resolution mode, acquisition time of 0 to 10 min, ESI source, mass range of 100 to 1200 Da, scan time of 0.2 s^{-1}. The positive mode ESI conditions were 1.2 kV capillary voltage, 30 V cone voltage, 100 °C source temperature, desolvation temperature of 450 °C, 50 L h^{-1} cone gas flow, and 750 L h^{-1} desolvation gas flow. For internal calibration, a solution of leucine enkephalin (Sigma) 200 pg mL^{-1}, infused by the lock-mass probe with a flow rate of 10 μL min^{-1}, was used. UPLC-QToF-MS analyses were performed using a BEH C_{18} column (dimensions: 2.1 × 100 mm, 1.7 μm; Waters Corporation) and a mobile phase consisting of Milli-Q + 0.1% formic acid (Panreac) and MeCN (Sigma) + 0.1% formic acid. The elution gradient used was from 90:10 of H_2O/MeCN to 100% MeCN for 7 min, maintained in 100% MeCN for 2 min and H_2O/MeCN (90:10) for 0.9 min with a flow rate of 0.50 mL min^{-1}. The column was maintained at a temperature of 40 °C, and the samples were maintained at 15 °C. Samples were diluted in MeOH at a concentration of 0.01 mg mL^{-1}. HPLC-UV-MS analysis was carried out on a Waters chromatography system consisting of a Waters 2695 Alliance control system coupled to a Waters 2696 UV−visible spectrophotometric detector with photodiode array detector, connected sequentially to a Waters Micromass ZQ 2000 mass spectrometry detector operated using an Empower platform. Analyses were performed using a Waters C_{18} X-Terra reversed-phase column (4.6 × 250 mm, 5 mm). The mass spectrometer detector was

DOI: 10.1021/acs.jnatprod.9b00635
J. Nat. Prod. XXXX, XXX, XXX−XXX

optimized using the following conditions: capillary voltage 3 kV; temperature of the source 100 °C; desolvation temperature 350 °C; ESI mode, acquisition range 150 to 1200 Da; gas flow without cone 50 L h $^{-1}$; desolvation gas flow 350 L h $^{-1}$. Samples were diluted in MeOH at a concentration of 2 mg mL^{-1}. Electronic circular dichroism spectra were measured on a JASCO J-810 spectropolarimeter using quartz cells (10 mm path length) at 23 °C.

***Penicillium solitum* IS1-A Strain Identification.** The fungus *Penicillium solitum* IS1-A was isolated from a marine sample (isopod) collected at King George Island (Admiralty Bay, Punta Plaza) at Maritime Antarctica during the Brazilian expedition in austral summer 2010 (OPERANTAR XXVIII).[64] The fungus was identified by molecular taxonomy (beta-tubulin sequencing and phylogeny). The sequence used in this study has been deposited in GenBank as the accession number MN365722. The fungus is maintained in the collection of the Laboratory of Environmental and Industrial Mycology associated with the Central of Microbial Resources of São Paulo State University, CRM-UNESP (UNESP, Rio Claro, SP, Brazil), under the accession number LAMAI 607.

Extraction and Isolation. *Penicillium solitum* IS1-A strain was grown in PDB medium. Five liters of PDB was incubated under static conditions. After 30 days fungal cultures were blended with EtOAc. The mixture of growth medium and EtOAc was shaken overnight, then filtered through a pad of Celite. The organic fraction was separated by decantation after liquid−liquid partitioning. The EtOAc fraction was evaporated, dried, solubilized in H_2O/MeOH 5:95 (v/v), and subjected to partition with hexane three times. The MeOH-soluble fraction was named AI (1.2 g). The H_2O fraction was extracted by a 1:1:1 mixture (500 g) of XAD-2, XAD-4, and XAD-7 macroporous polymeric resins with overnight shaking (160 rpm). The mixture of resins was then recovered by filtration and washed with H_2O, and the water-soluble organic material was desorbed with MeOH and with MeOH/acetone 50:50 (v/v) and evaporated. The water-soluble organic fraction (XI extract, 640.0 mg) was subjected to chromatographic separations, including phenyl-bonded silica gel and C_{18} reversed-phase column chromatography, Sephadex G-15 gel permeation chromatography, and C_{18}, C_8, and Ph HPLC purification (Supporting Information). Solitumine A (**1**, 55.5 mg), solitumine B (**2**, 7.2 mg), solitumine C (**3**, 9.9 mg), solitumidine B (**4**, 12.0 mg), solitumidine E (**5**, 8.0 mg), and solitumidine D (**6**, 9.0 mg) were obtained.

*Solitumine A (**1**):* greenish-yellow solid; $[\alpha]_D^{24}$ +377 (*c* 0.23, MeOH); UV (MeOH) λ_{max} nm (log ε) 214 (4.17), 240 (4.29), 262 (3.78), 396 (3.52); IR (neat) ν_{max} 3327, 3084, 2963, 1639, 1614, 1525, 1340, 1240, 1029 cm^{-1}; ^{1}H and ^{13}C NMR data, Table 1; HRESITOFMS *m*/*z* 374.2079 [M + H]$^+$ (calcd for $C_{20}H_{27}N_3O_4$, 374.2074).

*Solitumine B (**2**):* yellowish-white solid; $[\alpha]_D^{24}$ −11.5 (*c* 0.26, MeOH); UV (MeOH) λ_{max} nm (log ε) 214 (4.12), 240 (4.04), 247 (3.99), 318 (3.59), 330 (3.61); IR (neat) ν_{max} 3400, 2947, 2835, 1674, 1627, 1201, 1141, 1026 cm^{-1}; ^{1}H and ^{13}C NMR data, Table 1; HRESITOFMS *m*/*z* 372.1922 [M + H]$^+$ (calcd for $C_{20}H_{25}N_3O_4$, 372.1918).

*Solitumidine A (**3**):* brown solid; $[\alpha]_D^{24}$ −8.1 (*c* 0.46, MeOH); UV (MeOH) λ_{max} nm (log ε) 225 (4.28), 283 (3.63), 291 (3.59); IR (neat) ν_{max} 3400, 2947, 2835, 1674, 1627, 1201, 1141, 1026 cm^{-1}; ^{1}H and ^{13}C NMR data, Table 2; HRESITOFMS *m*/*z* 358.2139 [M + H]$^+$ (calcd for $C_{20}H_{27}N_3O_3$, 358.2125).

*Solitumidine B (**4**):* brown solid; $[\alpha]_D^{24}$ −55 (*c* 0.40, MeOH); UV (MeOH) λ_{max} (log ε) 202 (4.21), 224 (4.07), 283 (3.45), 291 (3.40) nm; IR (neat) ν_{max} 3415, 2960, 2845, 1715. 1640, 1520, 1020 cm^{-1}; ^{1}H and ^{13}C NMR data, Table 2; HRESITOFMS *m*/*z* 359.1968 [M + H]$^+$ (calcd for $C_{20}H_{26}N_2O_4$, 359.1965).

*Solitumidine C (**5**):* yellowish-brown solid; $[\alpha]_D^{24}$ −45 (*c* 0.26, MeOH); UV (MeOH) λ_{max} nm (log ε) 208 (4.18), 251 (3.59), 285 (3.03); IR (neat) ν_{max} 3277, 3088, 2970, 2885, 1693, 1616, 1473, 1338, 1234, 1010, 760 cm^{-1}; ^{1}H and ^{13}C NMR data, Table 2; HRESITOFMS *m*/*z* 374.2077 [M + H]$^+$ (calcd for $C_{20}H_{27}N_3O_4$, 374.2074).

*Solitumidine D (**6**):* brown solid; $[\alpha]_D^{24}$ −9 (*c* 0.13, MeOH); UV (MeOH) λ_{max} nm (log ε) 231 (4.15), 234 (4.14), 261 (3.77), 327 (3.43) nm; IR (neat) ν_{max} 3408, 3093,2978, 1730, 1658, 1583, 1521, 1444, 1203 cm^{-1}; ^{1}H and ^{13}C NMR data, Table 3; HRESITOFMS *m*/*z* 390.2010 [M + H]$^+$ (calcd for $C_{20}H_{27}N_3O_4$, 390.2023).

Acid Hydrolysis and Marfey's Analysis. Approximately 0.5 mg of each compound was subjected to hydrolysis with 6 N HCl (1 mL) at 100−110 °C for about 24 h. After hydrolysis, residual HCl was removed by resuspending the samples with H_2O and applying to repeated evaporation in a SpeedVac system. The hydrolysate as well as amino acid standards were derivatized with L-Marfey's reagent (*N*-(2,4-dinitro-5-fluorophenyl)alaninamide, L-FDAA). Approximately 0.1 mg of the hydrolysate or standards was mixed with 80 μL of acetone, 50 μL of H_2O, 20 μL of 0.5 N $NaHCO_3$, and 20 μL of L-FDAA solution (10 mg/mL in acetone). The mixtures were stirred at 40 °C for 1 h. After that, the mixtures were removed from heat and quenched with 16 μL of 0.5 N HCl. Reaction mixtures were evaporated and resuspended in MeOH for HPLC-UV-MS analysis. Analyses were performed using a Waters C_{18} X-Terra reversed-phase column (4.6 × 250 mm, 5 mm), with a linear gradient of H_2O (A) and MeOH (B) both with 0.1% formic acid. This elution program went from 10% to 100% of (B), over 20 min. Extracted UV chromatograms at λ_{max} 340 nm and retention times were compared for each Marfey's derivative for the assignment of absolute configuration.[65]

Vibrational Circular Dichroism Calculations. Conformational searches were carried out at the molecular mechanics level of theory with the Monte Carlo algorithm employing the MM+ force field incorporated in the HyperChem 8.0.10 software package. Calculations were performed for the arbitrarily chosen (2*S*,3*R*,19*S*)-, (2*R*,3*R*,19*S*)-, and (2*R*,3*S*,19*S*)-**1**, as well as (3*R*,19*S*)- and (3*S*,19*S*)-**5**. Initially, 76 conformers of (2*S*,3*R*,19*S*)-**1** with relative energy (rel E.) within 10 kcal mol^{-1} of the lowest-energy conformer were selected and further geometry optimized at the B3LYP/PCM(DMSO)/6-31G(d) level. The nine conformers with rel E. < 1.89 kcal mol^{-1}, which corresponded to more than 85% of the total Boltzmann distribution, were selected for IR and VCD spectral calculations. Conformers of the (2*R*,3*S*,19*S*)-**1** stereoisomer were constructed from the nine lowest-energy conformers identified for (2*S*,3*R*,19*S*)-**1**. After inversion of the C-19 stereocenter, geometry optimizations steps and vibrational analysis were performed at the B3LYP/PCM(DMSO)/6-31G(d) level. Out of nine conformers, four with rel E. < 2.2 kcal mol^{-1} were used for IR and VCD spectral calculations. The final VCD spectrum was obtained by multiplying the Boltzmann-averaged spectra obtained for (2*S*,3*R*,19*R*)-**1** by (−1). As for the epimer (2*R*,3*R*,19*S*)-**1**, 124 conformers with relative energy (rel E.) within 10 kcal mol^{-1} of the lowest-energy conformer were selected and further geometry optimized at the B3LYP/PCM(DMSO)/6-31G(d) level. This larger number of conformers included ring puckering possible for the dihydroquinolin-4(1*H*)-one moiety that would support the ^{1}H NMR data. The six conformers with rel E. < 1.97 kcal mol^{-1}, which corresponded to more than 87% of the total Boltzmann distribution, were selected for IR and VCD spectral calculations. As for (3*R*,19*S*)-**5**, 63 conformers with rel E. within 10 kcal mol^{-1} of the lowest-energy conformer were selected and further geometry optimized at the B3LYP/PCM(DMSO)/6-31G(d) level. The seven conformers with rel E. < 1.20 kcal mol^{-1}, which corresponded to more than 80% of the total Boltzmann distribution, were selected for IR and VCD spectral calculations. Finally, for (3*S*,19*S*)-**5**, 53 conformers with rel E. within 10 kcal mol^{-1} of the lowest-energy conformer were selected and further geometry optimized at the B3LYP/PCM(DMSO)/6-31G(d) level. Eight conformers with rel E. < 2.0 kcal mol^{-1}, which corresponded to more than 80% of the total Boltzmann distribution, were selected for IR and VCD spectral calculations. All DFT calculations were carried out at 298 K in DMSO solution using the polarizable continuum model (PCM) in its integral equation formalism version (IEFPCM) incorporated in Gaussian 09 software.[66] For the IR and VCD spectral simulations, the spectra were created using dipole and rotational strengths from Gaussian, which were calculated at the same level used during the geometry optimization

DOI: 10.1021/acs.jnatprod.9b00635
J. Nat. Prod. XXXX, XXX, XXX−XXX

step and converted into molar absorptivities (M^{-1} cm^{-1}). Each spectrum was plotted as a sum of Lorentzian bands with half-widths at half-maximum of 6 cm^{-1}. The calculated wavenumbers were multiplied with a scaling factor of 0.975. The final spectra were generated according to Boltzmann weighting of the lowest-energy conformers identified for each group of molecules and plotted using Origin 8 software.

■ ASSOCIATED CONTENT

Supporting Information

The Supporting Information is available free of charge at https://pubs.acs.org/doi/10.1021/acs.jnatprod.9b00635.

Literature reports on the isolation of fungal metabolites using adsorptive extraction procedures (2008−2018), bioassay procedures, isolation procedures and schemes, quantification of solitumine A extraction using XAD resins, HPLC traces of Marfey analyses, HRMS, UV, IR, ECD, VCD, ^{1}H and ^{13}C NMR, and selected 2D NMR spectra of compounds **1**−**6** (PDF)

■ AUTHOR INFORMATION

Corresponding Author

*Tel: +55-16-33739954. Fax: +55-16-33739952. E-mail: rgsberlinck@iqsc.usp.br.

ORCID

João M. Batista, Jr.: 0000-0002-0267-2631

Carlos H. G. Martins: 0000-0001-8634-6878

Roberto G. S. Berlinck: 0000-0003-0118-2523

Author Contributions

#J. P. G. Rodríguez and D. I. Bernardi contributed equally.

Notes

The authors declare no competing financial interest.

■ ACKNOWLEDGMENTS

The authors thank V. A. Venâncio and D. Tomazela for assistance in initial screening efforts, as well as Dr. S. Franzblau and Dr. B. Wan (Institute for Tuberculosis Research, College of Pharmacy, University of Illinois at Chicago) for performing the anti-TB assays. Financial support was provided by São Paulo State Funding Agency, Brazil (BIOTA/BIOprospecTA FAPESP grant 2013/50228-8 to RGSB; FAPESP grant 2014/25222-9 to JMBJ, FAPESP scholarships 2016/21341-9 to D.I.B., 2017/06014-4 to J.R.G., 2013/23153-7 to R.P.M.U., 2016/16033-3 to J.I.Q.B.), CAPES, Brazil (to J.P.G.R., J.M.O., and A.F.B.). This research was also supported by resources supplied by the Centre for Scientific Computing (NCC/GridUNESP) of São Paulo State University (UNESP).

■ REFERENCES

(1) Pye, C. R.; Bertin, M. J.; Lokey, R. S.; Gerwick, W. H.; Linington, R. G. *Proc. Natl. Acad. Sci. U. S. A.* **2017**, *114*, 5601−5606.

(2) Ióca, L. P.; Allard, P.-M.; Berlinck, R. G. S. *Nat. Prod. Rep.* **2014**, *31*, 646−675.

(3) Kong, D.; Guo, M.; Xiao, Z.; Chen, L.; Zhang, H. *Chem. Biodiversity* **2011**, *8*, 1968−1977.

(4) Bernardi, D. I.; Chagas, F. O.; Monteiro, A. F.; Santos, G. F.; Berlinck, R. G. S. *Prog. Chem. Org. Nat. Comp.* **2019**, *108*, 207.

(5) Hug, J. J.; Bader, C. D.; Remškar, M.; Cirnski, K.; Müller, R. *Antibiotics* **2018**, *7*, 44.

(6) Berlinck, R. G. S.; Monteiro, A. F.; Bertonha, A. F.; Bernardi, D. I.; Gubiani, J. R.; Slivinski, J.; Michaliski, L. F.; Tonon, L. A. C.; Venancio, V. A.; Freire, V. F. *Nat. Prod. Rep.* **2019**, *36*, 981.

(7) Harvey, A. L.; Edrada-Ebel, R.; Quinn, R. J. *Nat. Rev. Drug Discovery* **2015**, *14*, 111−129.

(8) Harvey, A. L.; Clark, R. L.; Mackay, S. P.; Johnston, B. F. *Expert Opin. Drug Discovery* **2010**, *5*, 559−568.

(9) Newman, D. J. *Front. Microbiol.* **2016**, *7*, 1832.

(10) Masschelein, J.; Jennera, M.; Challis, G. L. *Nat. Prod. Rep.* **2017**, *34*, 712−783.

(11) Still, P. C.; Johnson, T. A.; Theodore, C. M.; Loveridge, S. T.; Crews, P. *J. Nat. Prod.* **2014**, *77*, 690−702.

(12) Son, S.; Hong, Y.-S.; Futamura, Y.; Jang, M.; Lee, J. K.; Heo, K. T.; Ko, S. K.; Lee, J. S.; Takahashi, S.; Osada, H.; Jang, J. H.; Ahn, J. S. *Org. Lett.* **2018**, *20*, 7234−7238.

(13) Lu, S.; Nishimura, S.; Hirai, G.; Ito, M.; Kawahara, T.; Izumikawa, M.; Sodeoka, M.; Shin-ya, K.; Tsuchida, T.; Kakeya, H. *Chem. Commun.* **2015**, *51*, 8074−8077.

(14) Hoshino, S.; Okada, M.; Awakawa, T.; Asamizu, S.; Onaka, H.; Abe, I. *Org. Lett.* **2017**, *19*, 4992−4995.

(15) Schorn, M. A.; Alanjary, M. M.; Aguinaldo, K.; Korobeynikov, A.; Podell, S.; Patin, N.; Lincecum, T.; Jensen, P. R.; Ziemert, N.; Moore, B. S. *Microbiology* **2016**, *162*, 2075−2086.

(16) Kingston, D. G. I. *J. Nat. Prod.* **2011**, *74*, 496−511.

(17) Jakubczyk, D.; Cheng, J. Z.; O'Connor, S. E. *Nat. Prod. Rep.* **2014**, *31*, 1328−1338.

(18) For a short list of selected examples of natural products with novel carbon skeletons isolated from Chinese plants, see: (a) Fan, Y. Y.; Sun, Y. L.; Zhou, B.; Zhao, J. X.; Sheng, L.; Li, J. Y.; Yue, J. M. *Org. Lett.* **2018**, *20*, 5435−5438. (b) Ding, C.-F.; Ma, H.-X.; Yang, J.; Qin, X.-J.; Njateng, G. S. S.; Yu, H. F.; Wei, X.; Liu, Y. P.; Huang, W.-Y.; Yang, Z.-F.; Wang, X.-H.; Luo, X.-D. *Org. Lett.* **2018**, *20*, 2702−2706. (c) He, Q.-F.; Wu, Z.-L.; Huang, X.-J.; Zhong, Y.-L.; Li, M.-M.; Jiang, R.-W.; Li, Y.-L.; Ye, W.-C.; Wang, Y. *Org. Lett.* **2018**, *20*, 876−879. (d) Zhang, C. L.; Liu, Y. F.; Wang, Y.; Liang, D.; Jiang, Z. B.; Li, L.; Hao, Z. Y.; Luo, H.; Shi, G. R.; Chen, R. Y.; Cao, Z. Y.; Yu, D. Q. *Org. Lett.* **2015**, *17*, 5686−5689. (e) Zhang, H.; Zhu, K. K.; Han, Y. S.; Luo, C.; Wainberg, M. A.; Yue, J. M. *Org. Lett.* **2015**, *17*, 6274−6277.

(19) Hooper, I. R. In *Aminoglycoside Antibiotics*; Umezawa, H., Hooper, I. R., Eds.; Springer-Verlag: Berlin, 1982; pp 1−35.

(20) Shimizu, Y. *J. Nat. Prod.* **1985**, *48*, 223−235.

(21) Quinn, R. J. In *Bioorganic Marine Chemistry*; Scheuer, P. J., Ed.; Springer-Verlag: Berlin, 1988; Vol. *2*, pp 1−41.

(22) Shimizu, Y. In *Natural Products Isolation*; Cannell, R. J. P., Ed.; Humana Press: Totowa, 1998; pp 329−342.

(23) Wright, A. E. In *Natural Products Isolation*; Cannell, R. J. P., Ed.; Humana Press: Totowa, 1998; pp 365−408.

(24) Shimizu, Y.; Li, B. In *Natural Products Isolation*, 2nd ed.; Sarker, S. D., Latif, Z., Gray, A. I., Eds.; Humana Press: Totowa, 2006; pp 415−438.

(25) Jandera, P.; Janas, P. *Anal. Chim. Acta* **2017**, *967*, 12−32.

(26) Guo, Y. *Analyst* **2015**, *140*, 6452−6466.

(27) Wang, L. J.; Wei, W. L.; Xia, Z. N.; Jie, X.; Xia, Z. Z. L. *TrAC, Trends Anal. Chem.* **2016**, *80*, 495−506.

(28) Cardellina, J. H.; Munro, M. H. G.; Fuller, R. W.; Manfredi, K. P.; McKee, T. C.; Tischler, M.; Bokesch, H. R.; Gustafson, K. R.; Beutler, J. A.; Boyd, M. R. *J. Nat. Prod.* **1993**, *56*, 1123−1129.

(29) Månsson, M.; Phipps, R. K.; Gram, L.; Munro, M. H. G.; Larsen, T. O.; Nielsen, K. F. *J. Nat. Prod.* **2010**, *73*, 1126−1132.

(30) Espada, A.; Anta, C.; Bragado, A.; Rodríguez, J.; Jiménez, C. *J. Chromat. A* **2011**, *1218*, 1790−1794.

(31) Le Ker, C.; Petit, K.-E.; Biard, J.-F.; Fleurence, J. *Mar. Drugs* **2011**, *9*, 82−9.

(32) Worthen, D. R.; Jay, M.; Bummer, P. M. *Drug Dev. Ind. Pharm.* **2001**, *27*, 277−286.

(33) Dawson, M. J.; Farthing, J. E.; Marshall, P. S.; Middleton, R. F.; O'Neill, M. J.; Shuttleworth, A.; Stylli, C.; Tait, R. M.; Taylor, P. M.; Wildman, H. G.; Buss, A. D.; Langley, D.; Hayes, M. V. *J. Antibiot.* **1992**, *45*, 639−647.

(34) Bergstrom, J. D.; Kurtz, M. M.; Rew, D. J.; Amend, A. M.; Karkas, J. D.; Bostedor, R. D.; Bansal, V. S.; Dufresne, C.; VanMiddlesworth, F. L.; Hensens, O. D.; Liesch, J. M.; Zink, D. L.;

DOI: 10.1021/acs.jnatprod.9b00635
J. Nat. Prod. XXXX, XXX, XXX−XXX

Wilson, K. E.; Onishi, J.; Milligan, J. A.; Bills, G.; Kaplan, L.; Omstead, M. N.; Jenkins, R. G.; Huang, L.; Meinz, M. S.; Quinn, L.; Burg, R. W.; Kong, Y. L.; Mochales, S.; Mojena, M.; Martin, L.; Pelaez, F.; Diez, M. T.; Alberts, A. W. *Proc. Natl. Acad. Sci. U. S. A.* **1993**, *90*, 80−84.
(35) Metcalf, W. W.; van der Donk, W. A. *Annu. Rev. Biochem.* **2009**, *78*, 65−94.
(36) Crüsemann, M.; O'Neill, E. C.; Larson, C. B.; Melnik, A. V.; Floros, D. J.; Silva, R. R.; Jensen, P. R.; Dorrestein, P. C.; Moore, B. S. *J. Nat. Prod.* **2017**, *80*, 588−597.
(37) Bal, D.; Gradowska, W.; Gryff-Keller, A. *J. Pharm. Biomed. Anal.* **2002**, *28*, 1061−1071.
(38) Bal, D.; Gryff-Keller, A. *Magn. Reson. Chem.* **2002**, *40*, 533−536.
(39) Lee, J.; Yoon, H.-R. *Anal. Lett.* **2015**, *48*, 231−240.
(40) Li, J.; Chase, H. A. *Nat. Prod. Rep.* **2010**, *27*, 1493−1510.
(41) Yang, K.; Qi, L.; Wei, W.; Wu, W.; Lin, D. *Environ. Sci. Pollut. Res.* **2016**, *23*, 1060−1070.
(42) Lin, S.-H.; Juang, R.-S. *J. Environ. Manage.* **2009**, *90*, 1336−1349.
(43) Abdullah, M. A.; Chiang, L.; Nadeem, M. *Chem. Eng. J.* **2009**, *146*, 370−376.
(44) Wessels, P.; Gohrt, A.; Zeeck, A.; Drautz, H.; Zahner, H. *J. Antibiot.* **1991**, *44*, 1013−1018.
(45) Grabley, S.; Hammann, P.; Hutter, K.; Kirsch, R.; Kluge, H.; Thiericke, R.; Mayer, M.; Zeeck, A. *J. Antibiot.* **1992**, *45*, 1176−1181.
(46) Grabley, S.; Hammann, P.; Kluge, H.; Wink, J.; Kricke, P.; Zeeck, A. *J. Antibiot.* **1991**, *44*, 797−800.
(47) Arslanian, R. L.; Parker, C. D.; Wang, P. K.; McIntire, J. R.; Lau, J.; Starks, C.; Licari, P. J. *J. Nat. Prod.* **2002**, *65*, 570−572.
(48) Chehade, C. C.; Dias, R. L. A.; Berlinck, R. G. S.; Ferreira, A. G.; Costa, L. V.; Rangel, M.; Malpezzi, E. L. A.; Freitas, J. C.; Hajdu, E. *J. Nat. Prod.* **1997**, *60*, 729−731.
(49) Britton, R.; de Oliveira, J. H. H. L.; Andersen, R. J.; Berlinck, R. G. S. *J. Nat. Prod.* **2001**, *64*, 254−255.
(50) Santos, M. F. C.; Harper, P. M.; Williams, D. E.; Mesquita, J. T.; Pinto, E. G.; Costa-Silva, T. A.; Hajdu, E.; Ferreira, A. G.; Santos, R. A.; Murphy, P. J.; Andersen, R. J.; Tempone, A. G.; Berlinck, R. G. S. *J. Nat. Prod.* **2015**, *78*, 1101−1112.
(51) Rodriguez, J. P. G.; Williams, D. E.; Sabater, I. D.; Bonugli-Santos, R. C.; Sette, L. D.; Andersen, R. J.; Berlinck, R. G. S. *RSC Adv.* **2015**, *5*, 66360−66366.
(52) Nicacio, K. J.; Ióca, L. P.; Fróes, A. M.; Leomil, L.; Appolinario, L. R.; Thompson, C. C.; Thompson, F. L.; Ferreira, A. G.; Williams, D. E.; Andersen, R. J.; Eustaquio, A. S.; Berlinck, R. G. S. *J. Nat. Prod.* **2017**, *80*, 235−240.
(53) Lau, J.; Frykman, S.; Regentin, R.; Ou, S.; Tsuruta, H.; Licari, P. *Biotechnol. Bioeng.* **2002**, *78*, 280−288.
(54) Blunt, J. W.; Calder, V. L.; Fenwick, G. D.; Lake, R. J.; McCombs, J. D.; Munro, M. H. G.; Perry, N. B. *J. Nat. Prod.* **1987**, *50*, 290−292.
(55) Wagenaar, M. M. *Molecules* **2008**, *13*, 1406−1426.
(56) Quinn, R. J. In *Chemical Genomics*; Fu, H., Ed.; Cambridge University Press: New York, 2012; pp 87−98.
(57) Suzuki, H.; Izuka, S.; Minami, H.; Miyakawa, N.; Ishihara, S.; Kumagai, H. *Appl. Environ. Microbiol.* **2003**, *69*, 6399−6404.
(58) Suzuki, H.; Yamada, C.; Kato, K. *Amino Acids* **2007**, *32*, 333−340.
(59) Simbirtsev, A.; Kolobov, A.; Zabolotnych, N.; Pigareva, N.; Konusova, V.; Kotov, A.; Variouchina, E.; Bokovanov, V.; Vinogradova, T.; Vasilieva, S.; Tuthil, C. *Russ. J. Immunol.* **2003**, *8*, 11−22.
(60) Adkins, D.; Suen, J. Y.; Sonis, S. T.; Modelska, K.; Tuthill, C. W.; Rios, I. *J. Clin. Oncol.* **2010**, *28*, e19693.
(61) Tuthill, C. W.; Papkoff, J.; Watkins, B. A.; Sonis, S. T. *J. Clin. Oncol.* **2011**, *29*, 5592.
(62) Saini, M.; Bindal, S.; Gupta, R. *Enzyme Microb. Technol.* **2017**, *99*, 67−76.
(63) Thornburg, C. C.; Britt, J. R.; Evans, J. R.; Akee, R. K.; Whitt, J. A.; Trinh, S. K.; Harris, M. J.; Thompson, J. R.; Ewing, T. L.; Shipley, S. M.; Grothaus, P. G.; Newman, D. J.; Schneider, J. P.; Grkovic, T.; O'Keefe, B. R. *ACS Chem. Biol.* **2018**, *13*, 2484−2497.
(64) Duarte, A. W. F.; Barato, M. B.; Nobre, F. S.; Polezel, D. A.; Oliveira, T. B.; Santos, J. A.; Rodrigues, A.; Sette, L. D. *Polar Biol.* **2018**, *41*, 2511.
(65) Crnkovic, C. M.; Krunic, A.; May, D. S.; Wilson, T. A.; Kao, D.; Burdette, J. E.; Fuchs, J. R.; Oberlies, N. H.; Orjala, J. *J. Nat. Prod.* **2018**, *81*, 2083−2090.
(66) Frisch, M. J.; Trucks, G. W.; Schlegel, H. B.; Scuseria, G. E.; Robb, M. A.; Cheeseman, J. R.; Scalmani, G.; Barone, V.; Mennucci, B.; Petersson, G. A.; Nakatsuji, H.; Caricato, M.; Li, X.; Hratchian, H. P.; Izmaylov, A. F.; Bloino, J.; Zheng, G.; Sonnenberg, J. L.; Hada, M.; Ehara, M.; Toyota, K.; Fukuda, R.; Hasegawa, J.; Ishida, M.; Nakajima, T.; Honda, Y.; Kitao, O.; Nakai, H.; Vreven, T.; Montgomery, J. A.; Peralta, J. E.; Ogliaro, F.; Bearpark, M.; Heyd, J. J.; Brothers, E.; Kudin, K. N.; Staroverov, V. N.; Kobayashi, R.; Normand, J.; Raghavachari, K.; Rendell, A.; Burant, J. C.; Iyengar, S. S.; Tomasi, J.; Cossi, M.; Rega, N.; Millam, N. J.; Klene, M.; Knox, J. E.; Cross, J. B.; Bakken, V.; Adamo, C.; Jaramillo, J.; Gomperts, R.; Stratmann, R. E.; Yazyev, O.; Austin, A. J.; Cammi, R.; Pomelli, C.; Ochterski, J. W.; Martin, R. L.; Morokuma, K.; Zakrzewski, V. G.; Voth, G. A.; Salvador, P.; Dannenberg, J. J.; Dapprich, S.; Daniels, A. D.; Farkas, Ö.; Foresman, J. B.; Ortiz, J. V.; Cioslowski, J.; Fox, D. J. *Gaussian 09, Revision A.02*; Gaussian: Wallingford, CT, 2009.

DOI: 10.1021/acs.jnatprod.9b00635
J. Nat. Prod. XXXX, XXX, XXX−XXX